Responses to NRC Request for Additional Information for Westinghouse Electric Company Topical Report WCAP-17794-P/WCAP-17794-NP, Revision 0, "10x10 SVEA Fuel Critical Power Experiments and New CPR Correlation: D5 for SVEA-96 Optima3" (Non-Proprietary)

August 2016

Westinghouse Electric Company
1000 Westinghouse Drive
Cranberry Township, PA 16066

1. RAI-SNPB-01 Reference for Test Facility

Provide appropriate references which describe the test facility in greater detail and the Quality Assurance program applied.

Response:

The main features of the FRIGG facility are described in Section 3 of WCAP-17794-P. The general requirements for performing tests at this facility are provided in BTA 07-0885, "FRIGG dryout measurements and evaluation." The measurement system FRIGG95 is described in detail in NL 95-127, "Functional specifications: Test Loop FRIGG 95" (in Swedish). The procedures applied by the laboratory staff before, during and after measurements are described in BTP 01-028, "FRIGG - Routines for performing the tests" (QA-manual in Swedish) and BUP 99-075, "FRIGG – Instructions for Operation" (in Swedish).

Westinghouse's QA program is in compliance with the requirements in Appendix B to 10 CFR Part 50 and has been audited by the NRC.

According to these instructions, following each of the three measurement campaigns for the SVEA 96 Optima3, a quality assessment was performed to verify the accuracy of all measured parameters. The results are documented in internal Westinghouse reports. For the measurements with cosine power shaped rods, this is described in BTA 05-249, "FRIGG – Test SF24XC-Mesurement results" (in Swedish).

The documents are internal Westinghouse documents and can be made available for NRC review on request.

2. RAI-SNPB-02 Validation for Test Facility

Demonstrate that the FRIGG test facility has been validated by comparison to experimental results from an outside source (i.e., benchmarks).

Response:

As part of a Technical Development Agreement between ASEA-ATOM (AA) and General Electric (GE), a series of comparative full-scale dryout experiments were performed at the AA FRIGG and GE ATLAS loop facilities during the late 1970's. Comparisons between FRIGG and ATLAS data, and between correlations based on the corresponding data, were made. The data included measurements of critical power and pressure drop. The measurement procedures were those specific to each test facility.

One important objective was to duplicate the same test conditions (bundle geometry, heat flux distribution and spacer design) as far as realistically possible, make a direct comparison of the measured critical power levels and look for evidence of any laboratory bias or trends. This was the particular objective of the Program Statement AAGE-104 where a 16-rod bundle tested by GE in the ATLAS loop was duplicated and tested by AA in the FRIGG loop. The selected bundle was a 4×4 subset of the 7×7 lattice type with corner peaking and cosine axial heat flux distribution. The same spacers were applied in the two tests. The experimental procedures were, as far as possible, the same as applied in large bundle tests. Direct comparison of the measured critical power levels showed very consistent trends. [ ]^{a,c} A discrepancy of that order could well be explained by the combined measurement errors in the two series of experiments and, hence, it was concluded that there was no evidence of any laboratory bias.

3. RAI-SNPB-03 Plots for Range of Parameters

Provide plots similar to Figures 4-5 through 4-8 which demonstrate that the typical application range is bounded by the experimental data. This should include plots of Pressure vs. R-factor and Inlet Subcooling vs. R-factor. These plots should identify the domain of the Typical Application as well as the domain of the limits of the D5 correlation (i.e., the computational domain).

Response:

The requested plots, along with the domain of typical application and the domain of D5 applicability, are provided below.

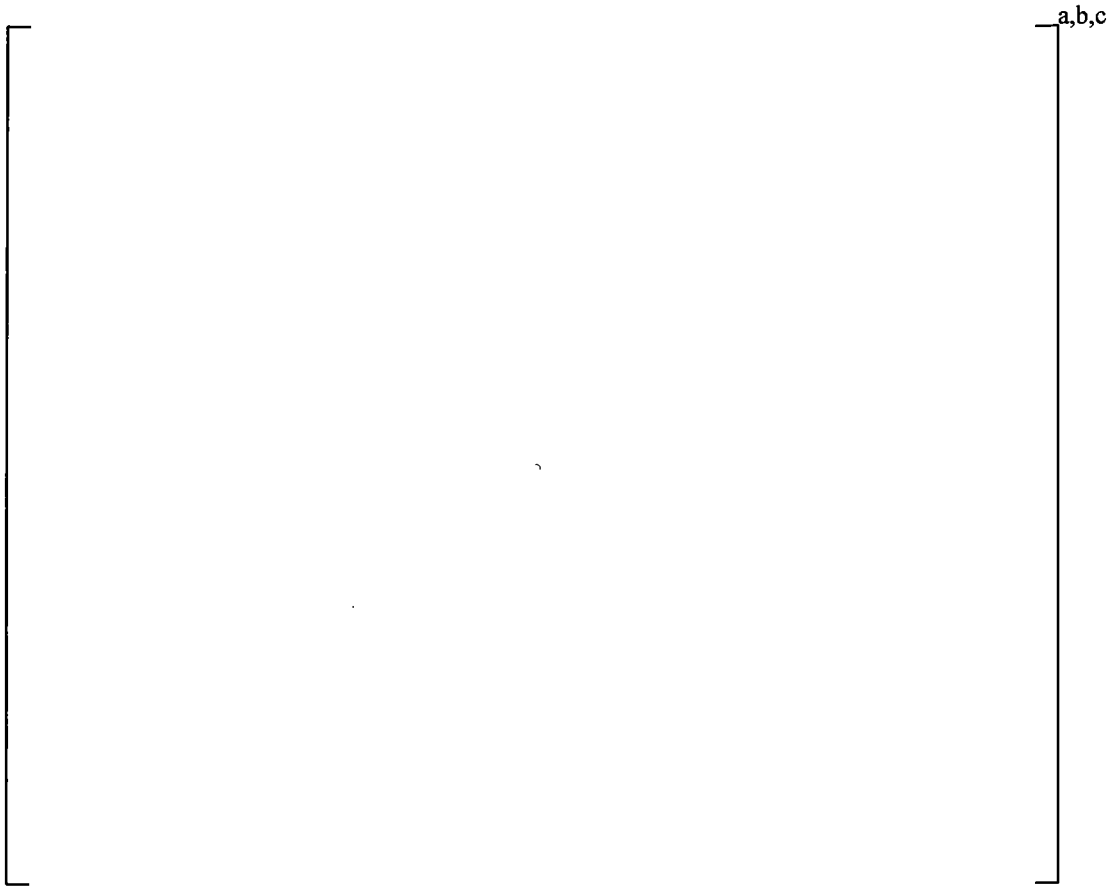

[a,b,c]

4. RAI-SNPB-04 Difference in dimensions between fuel and test bundle

Provide a more detailed description about the difference between the fuel bundle and the test bundle, as quantified in Figure 3-4 of the TR. Discuss the cause of these differences, how these differences were addressed, and any impact of these differences.

Response:

For the following geometrical parameters there were differences between the test bundles and typical nominal dimensions of the fuel in reactor.

Heated length and spacer positions

SVEA-96 Optima3 is aimed to be supplied to reactors with different heated lengths. In all cases [

]^{a,c} This case is applicable to GE BWR 4-6 type plants. This means that for the slightly shorter fuel in GE BWR 2-3 plants, [ ]^{a,c} compared to the test bundle. [

]^{a,c}

In addition to the [ ]^{a,c} This small effect is fully captured by the I_2 concept of the D5 correlation.

The mechanical lengths of the part-length rods are the same in all reactor fuel bundles since they are coupled to the positions of the spacer levels. The same physical lengths were used in the test bundles. The [

]^{a,c} This means that there can be minor differences in the [ ]^{a,c} Since dryout typically occurs well above the part-length rods this effect is judged to be insignificant.

Flow area

The flow area of the test channel is slightly smaller than that of the fuel bundle. The difference is in the corners where the water cross walls are welded to the outer channel section. The inner dimensions of the channel are however the same. The impact of the small difference in flow area is fully captured in the mass flux that is calculated as input to the D5 correlation. The rod pitch, which is important for dryout performance, is not impacted.

5. RAI-SNPB-05 Difference in grid spacer types between fuel and test bundle

Provide justification that the differences between the grid spacers used in the test bundle and those used in the reactor fuel bundle will not impact the flow field. Further, provide details as to why different spacers were used. Specifically justify the use of SP1-XA spacer.

Response:

There is no difference between the spacer grid types used in the test bundle and those used in the reactor fuel bundle. However, [

]^{a,c} This is described in Section 3.2. [

]^{a,c}

6. RAI-SNPB-06 Axial Shift in Grid Spacers

Provide a figure which contains the initial and final position of the axial grid spacers. Provide any results of state points which were repeated on the cosine power shape vs the date the data point was taken. Provide a plot of the error vs. date and time of data point for the cosine power tests. Provide further details on if the axial shift could have impacted the thermocouples measuring dryout (e.g., could the grid spacer move to cover the thermocouple and thus prevent dryout detection). In general, provide further analysis demonstrating that the axial shift does still results in a similar flow field for the tested bundle compared with the reactor fuel bundle.

Response:

The positions of the spacers before and after the experiment, along with the positions of the thermocouples (TCs), are shown in the figure below.

a,b,c

As stated in Section 4.4, the following spacer shifts were measured in mm, ("+" for downstream and "–" for upstream):

Spacer number	1	2	3	4	5	6	7	8
Axial shift (mm)	+1	+3	+29	+20	+25	-5	-10	+8

The spacers are numbered from the top, as defined in Figure 3-10.

In the full-length rods and 2/3-length rods, for which dryout was detected, the TCs were positioned immediately [ ]^{a,c} below the spacers at levels 1-5, as well as at the end of heated length (EHL) for both rod types. The TCs at EHL were positioned halfway between two spacers, approximately [ ]^{a,c} from the nearest spacer. As can be seen from the table above, the spacers moved upwards at the levels 1-5 where TCs were installed. Hence, the axial shift did not cause any TC to be covered by a spacer.

The above spacer shifts correspond to the following changes in spacer spans (distance between consecutive spacers):

[

] a,b,c

A change to a longer span ("+" change) conservatively reduces the dryout margin for that particular span. The spacer spans in SVEA-96 Optima3 are optimized to have [

]^{a,c} This performance can be seen, e.g., in Figure 4-29. A potential non-conservative improvement in margin below spacer 2, due to the span being reduced by 26 mm, would thus not have any significant impact on the critical power of the sub-bundle. It can also be noted in Appendix C that dryout often occurs at different axial levels simultaneously.

The MEFISTO code has been used to quantify the impact of the spacer shifts on critical power. The MEFISTO code is well-suited for this kind of analysis since the spacer effects are directly modeled by use of calibrated local (sub-channel specific) drop deposition enhancement factors applied downstream of each spacer. Critical power was predicted for the entire cosine database, with and without the spacer shifts. The relative critical power differences are plotted below as function of run number. Positive values correspond to larger critical power after the spacer shifts, which is potentially non-conservative. As mentioned above, the spacer shifts can lead to either increased or decreased critical power depending on whether the axial level of dryout occurs within an increased or reduced spacer span. The MEFISTO results show an average [

]^{a,c} Hence, it is concluded that the impact of spacer shifts are insignificant in relation to the conservatism included in the final correlation mean and standard deviation, see Section 6.3.3.

[a,b,c]

It is difficult to draw conclusions concerning the potential impact of spacer shifts on critical power from a plot of error vs. time of data point for the cosine database, since identical conditions were only repeated a few times and small prediction biases, e.g., between different radial power distributions, tend to introduce variation. [

]^{a,c}

[a,b,c]

7. RAI-SNPB-07 Radial Power Distributions

The NRC staff recognizes it is not realistically possible to test every possible combination of local powers, however, some methodology should be used to ensure that those combinations tested bound the possible local power distributions during transients and AOOs. Provide details of the methodology used by Westinghouse and justification that the combination of ***radial*** *powers tested bound the possible radial power distribution expected during normal operations and AOOs.*

Response:

When selecting the test matrix, particular emphasis was put on capturing the dependence of critical power (and quality) on the radial power distribution. The radial power distributions tested should cover relevant conditions experienced by fuel assemblies which have the possibility of being dryout limiting during normal operation as well as anticipated transients. Below, such relevant radial power distributions are discussed and compared to the corresponding selected test conditions in the FRIGG loop.

The radial heat flux distribution is not significantly altered during fast transients, i.e., in the present context it suffices to consider operation at steady-state and during quasi-stationary conditions. Under such conditions, the main sources of variation in radial power distribution are: 1) differences in nuclear design, i.e., distributions of U-235 enrichment and Gd concentration across the fuel rod lattice, including effects of isotopic depletion, 2) differences in inter-assembly water gaps between (S-, C- and D-lattice) plants, and 3) inserted control rods. In general, the emphasis in the selection of test conditions should be on assemblies that have the possibility of being dryout limiting for the core.

An important objective of the nuclear design optimization is to [

]^{a,c} Hence, as a result of the nuclear design process, [

]^{a,c} In order to simulate such limiting conditions, [

]^{a,c} were tested over the entire test matrix in FRIGG, i.e., for all combinations of axial power shape, flow, pressure, and subcooling. [

]^{a,c}

On the other hand, during the initial phase of Gd depletion the power is suppressed at and around the Gd rod locations which means that the fuel is usually not dryout limiting. [

]^{a,c}

Bundles adjacent to inserted control rods are usually not dryout limiting. [

]^{a,c}

[

]^{a,c} This process was repeated for all rods [

]^{a,c} and for all three axial power profiles.

[

]^{a,c}

8. RAI-SNPB-08 Axial Power Distributions

The NRC staff recognizes it is not realistically possible to test every possible combination of local powers, however, some methodology should be used to ensure that those combinations tested bound the possible local power distributions during transients and AOOs. Provide details of the methodology used by Westinghouse and justification that the combination of ***axial*** *powers tested bound the possible axial power distribution expected during normal operations and AOOs.*

Response:

The axial power distributions tested should cover relevant conditions experienced by fuel assemblies which can be potentially dryout limiting during normal operation as well as anticipated transients. Below, such relevant axial power distributions are discussed and compared to corresponding selected test conditions in the FRIGG loop.

At the beginning of cycle, during normal operation in a BWR, the axial power shape is shewed towards the bottom of the core as result of voiding. The core designer attempts to improve uranium utilization by making this bottom peak more pronounced and maintaining it as long as possible into the cycle. This increases the average void and allows more Pu-239 to be generated in the top of the core. Towards the end of cycle, when the power gradually shifts to the top of the core, the Pu-239 generated is utilized to increase reactivity and thereby prolong the cycle length. Disregarding the local influence of control rods, the level of peaking is typically more extreme in the bottom than in the top of the core. However, partially inserted control rods can locally enhance the top-peaked shape. During the transition from bottom to top-peaked, the power shape may resemble a chopped cosine, but is usually somewhat flatter.

In GE-type BWR plants with jet pumps (BWR 3-6) the Operating Limit Minimum CPR (OLMCPR) is typically set by a limiting pressure increase transient, such as the Generator Load Rejection Without Bypass (LRNBP) event. During pressure increase the void collapses in the top of the core which leads to positive reactivity insertion (due to the void coefficient being inherently negative). Hence, during the short time until the transient is terminated by a scram, the power moves towards the top of the core.

The heater rods used in FRIGG have fixed axial power shapes resulting from the manufacturing process. The bottom-peaked rods are turned upside down to obtain the top-peaked condition. The bottom-peaked power shape was chosen to simulate extreme, but realistic, bottom-peaked conditions that can be achieved during normal operation, early in the cycle. The resulting top-peaked power shape is representative of local conditions adjacent to partially inserted control rods as well as to conditions obtained in limiting pressure increase transients.

The data with cosine power shape mainly serve to test the ability of the CPR correlation to predict critical power for conditions that are in-between the extreme bottom and top-peaked shapes. [

]^{a,c}

9. RAI-SNPB-09 Part Length Fuel Rods

Provide a further discussion on the [

]^{a,c}

Response:

The mechanical lengths of the part-length rods are the same in all reactor fuel bundles since they are coupled to the positions of the spacer levels. The same mechanical lengths, with respect to the spacer grid elevations, were used in the test bundles.

[

]^{a,c}

In addition, [

]^{a,c}

10. RAI-SNPB-10 More Detailed Test Procedure

Provide a more detailed description of the test procedure. Specifically identify how each state point was reached including which system parameters were targeted first, second, etc.... Include the criteria for the stability of each type of data point (i.e., how much deviation in the system parameters would be needed to throw out a data point) as well as the criteria for determining when dryout has been observed. Provide these procedural details for both steady state and transient tests.

Response:

The targeted parameters were set in the following order: [ ]^{a,c} All parameters except total power are set first with a sufficient margin to critical power. After reaching stable conditions, the power is slowly increased until dryout is indicated by any thermocouple (TC). During the power increase, all other parameters are manually kept stable, and after a critical power indication, all parameters including power are kept stable for a recording. In the post processing, all recorded sample intervals are checked to assure that the conditions were stable. [ ]^{a,c}

Steady state dryout is assumed to occur for a minimum measured temperature rise of [ ]^{a,c} For power transients this criterion is slightly modified since the temperature rise due to the power increase needs to be considered, as described in section 7.3.4. The final assessment of dryout/non-dryout during transients is made by visually studying the temperature curves of limiting TCs.

11. RAI-SNPB-11 Reference for Test Procedure

Provide appropriate references for the test procedure.

Response:

The procedure manual, BTA 07-0885, "FRIGG dryout measurements and evaluation," describes the principles of critical power testing in the FRIGG loop. The test procedure is also described in each of the three test prospectuses. As an example, the measurements using rods with cosine axial power shape, the prospectus is BTU 05-069, "Dryout test in Frigg with sub-bundle for SVEA-96 Optima3 with new spacer SF24XC: Test program for steady-state measurements" (in Swedish).

The documents are internal Westinghouse documents, and can be made available for NRC review on request.

12. RAI-SNPB-12 Statistical Design of Experiments

Provide an explanation of methodology used to determine the values of experimental parameters where critical boiling transition measurements would be obtained. Specifically discuss the selection process in light of the general practices in statistical design of experiments where randomization is implemented to reduce any potential biases. Where could such practices be applied, where could such practices not be applied. Provide justification that the resulting statistics would still be applicable over the entire computational domain.

Response:

The database for each axial power profile consists of two main parts, one with variations of radial power distribution at nominal operating conditions (pressure ≈ 70 bar and sub-cooling ≈ 10 K), and one with variations of pressure and inlet sub-cooling for a few selected radial power distributions. In both parts, and for each radial power distribution, a series of flow levels were included. [

]^{a,c} For the parameter variation matrix, a randomization procedure was applied. The order in which the parameter combinations were tested was selected in a non-specific but structured way, by first randomly selecting the [

]^{a,c}

The above procedure is described in the procedure manual document BTA 07-0885, "FRIGG dryout measurements and evaluation." This document is an internal Westinghouse document and can be made available for NRC review on request.

13. RAI-SNPB-13 Mass Flux Uncertainty

[ ]^{a,c} *Generally, estimated accuracies are reported as ± X. Provide further clarification on the estimated accuracy of mass flux.*

Response:

The accuracy in mass flux is [ ]^{a,c}

14. RAI-SNPB-14 Other Means of Measurement

Provide details on the capability for diverse and redundant means of measuring the important experimental parameters including pressure, inlet mass flux, inlet temperature, and power.

Response:

[

]^{a,c}

15. RAI-SNPB-15 Instrumentation Calibration

Provide details on the instrumentation calibration, re-calibration, and verification. Include information on how often the instruments were calibrated and checked.

Response:

The instructions for calibration of the FRIGG instrumentation are defined in BUP 99-032, "User's instructions for the FRIGG measurement system" (in Swedish). In that document, all the instruments requiring calibrations are identified together with the specific requirements on the calibration to be performed prior to every measurement campaign. Check lists are also included to verify that the required calibrations have been performed and properly documented. The calibration is performed by qualified personal, who are also responsible for the calibration of equipment at the Westinghouse Electric Sweden Fuel Factory in Västerås.

All measurement equipment is calibrated [ ]^{a,c}

The above mentioned document is an internal Westinghouse document and can be made available for NRC review on request.

16. RAI-SNPB-16 Calculation of CPR Uncertainty

Provide further details on how the accuracy in the critical power of [ ]^{a,c} *was determined. Did this uncertainty contain the measurement uncertainties as well as any uncertainties caused by the procedure? How was the uncertainty in CPR calculated?*

Response:

In Section 3.5 the accuracies in the main variables defining the operating conditions in the experiment are discussed. There it is stated that the measurement uncertainties for those variables, when combined, give rise to an uncertainty in the critical power of about [ ]^{a,c} This is a conservative estimate. What that means is the following. If the CPR correlation model was "exact" (zero model uncertainty), the uncertainties in the input variables to the correlation and the uncertainty in the measured critical power would [

]^{a,c} was determined by standard error propagation based on the conservative estimates of the accuracies in the individual measurement variables given in Section 3.5.

17. RAI-SNPB-17 Experimental Uncertainty

Provide an analysis of repeated test points to estimate the experimental uncertainty in the CP value. Demonstrate that this uncertainty is small compared with the overall uncertainty in the critical boiling transition correlation.

Response:

An analysis of repeated test points was performed. [ ]^{a,c} from the SVEA-96 Optima3 dryout database were repeated during the test campaign (after running other dryout points over a time period of a few days). Various flows were considered [ ]^{a,c} While the variation in measured critical power from one test to the repeat test may depend on small differences in operating conditions, the variation in the calculated D5 CPR value (which equals predicted critical power / measured critical power) for nearly identical conditions mainly reflects the experimental uncertainty. Using this database, the standard deviation of D5 CPR variations was calculated to be [ ]^{a,c} experimental uncertainty reported in Section 3.5.

18. RAI-SNPB-18 Quantified Heat Losses

Provide an analysis which quantifies the heat losses in the test section and confirms the power measurement and power uncertainty is accurate.

Response:

The power losses were experimentally determined at the setup of the current FRIGG-loop. The values obtained were [ ]^{a,c}

Verification of heat balance is done at the beginning of each test campaign to make sure that the heat losses assumed in the analysis of the data are conservative. This verification is performed prior to the measurements campaign, as described in BTP 01-028, "FRIGG - Routines for performing the tests" (in Swedish), with the loop top-filled and a pressure being 20 bars higher that the saturation pressure for the actual outlet temperature to assure single-phase conditions. Once the FRIGG loop is at stable conditions, measurements with a sampling frequency of 1 Hz are performed for at least 100 s. The average values of the registered variables are utilized to evaluate the thermal power and electrical power.

The above mentioned document is an internal Westinghouse document and can be made available for NRC review on request.

19. RAI-SNPB-19 Derivation of the Transient Correlation

Provide additional details on the D5 transient correlation. [

]^{a,c}

Response:

The input parameters used to calculate the various components of the D5 CPR correlation (I_2 integral, R-factor, critical quality, critical power), for an arbitrary elevation z and arbitrary time t_{out}, are listed below. For each parameter, the time and location at which they are evaluated is provided. For simplicity, less relevant inputs (such as empirical constants) are not considered in this list.

For transient application, the transient is initiated at t_0 and at any considered time t_{out}, t_{in} is the time at which a fluid particle located at the outlet entered the bundle. For steady-state applications the time information is irrelevant (i.e., $t_0 = t_i = t_{out}$).

[

]^{a,c}

a,c

a,c

[

]a,c

[

]a,c

[

]a,c

a,c

I_2 integral concept

Motivation

The transformation of axial power profile, referred to herein as the I_2 integral, provides an improved method to capture the influence of the axial power distribution as compared with the local heat flux or the boiling length, as used in previous CPR correlations. The I_2 integral was first developed empirically and showed a behavior in reasonable agreement with experimental investigations of the effect of axial power distribution on dryout. Later, a theoretical justification was established by studying an idealized mechanistic theory. Under steady-state conditions, the I_2 parameter is defined at any axial position, z, above (downstream of) the boiling transition level, z_B, as

$$I_2(z) = \frac{1}{Lx(z)} \int_{z_B}^{z} x(z')dz' ,$$

where x is the axial distribution of steam quality and L is an arbitrary and constant reference length.

Assuming steady-state conditions (and ignoring possible thermal non-equilibrium) this is equivalent to

$$I_2(z) = \frac{1}{L} \frac{\int_{z_B}^{z} \int_{z_B}^{z'} q(z'')dz''dz'}{\int_{z_B}^{z} q(z')dz'}$$

where q is the axial distribution of heat flux.

Some interesting properties of I_2 are listed below.

- I_2 decreases with decreasing boiling length (i.e., with increasing inlet sub-cooling).
- For a uniform power distribution and saturated inlet (zero sub-cooling), $I_2 = 0.5$ at the outlet.
- For a saturated inlet, every power distribution which is symmetric around the channel mid-axial level will give $I_2 = 0.5$ at the outlet.
- Power distributions shifted towards the outlet will give smaller I_2 compared to inlet shifted ones.
- I_2 is insensitive to local flux spikes in agreement with the results of Groeneveld (Reference 19-1).
- I_2 at the outlet increases (linearly) as the cold patch in the experiments by Bennett *et al.* (Reference 19-2) is moved from the inlet towards the outlet, which is in qualitative agreement with the measured dryout power.

[

]^{a,c}

[

]^{a,c}

Earlier correlation concept vs. I_2

Numerous correlations of both quality/heat flux and quality/boiling length type have been developed, sometimes showing excellent agreement with extensive collections of experimental data. As long as complex parameters such as axial power distribution or geometry do not vary significantly, correlating the dryout power reduces to a regression problem in 3-4 dimensions depending on which parameters are included. Given enough experimental data, a solution to such a problem can be found with little consideration of the underlying physics. In fact it can be shown that, assuming uniform power distribution, the quality/heat flux, quality/boiling length and I_2 concepts are all fully equivalent.

The difference between the above concepts is mainly in the handling of the axial power distribution (geometry is usually not considered and will not be discussed here). The quality/heat flux model captures some important effects of the power distribution – mainly the reduced critical power for outlet peaked distributions and increased critical power for inlet peaked distributions. However, this concept also misses important aspects, such as being sensitive to local flux spikes and unable to appropriately predict the influence of the cold patch in the Bennet *et al.* experiments (Reference 19-2).

The quality/boiling length concept also captures the influence of the power distribution to some extent and is not sensitive to flux spikes. It is, however, [

]^{a,c}

The I_2 integral can be seen as a generalization of the boiling length concept as the integration range is exactly the boiling length. Thus, I_2 inherits the beneficial properties of the boiling length concept but at the same time accounts for the shape of the power distribution in the boiling part of the bundle. The I_2 variable correctly captures both the effects of upstream history and local variation in heat flux along the fuel bundle, properties that can only be obtained by combining all three variables of boiling length, annular length and local heat flux used in previous types of correlations. The I_2 integral is also able to capture the effect of the cold patch location in the experiments of Bennet *et al.* (Reference 19-2).

A comparison of the I_2 integral used in the D5 CPR correlation for SVEA-96 Optima3 fuel with the boiling length and annular length parameters used, e.g., in the CPR correlation for SVEA-96 Optima2 fuel is presented in the right panel of Figure 19-1 for two different axial power distributions shown schematically in the left panel. Since boiling length and annular length each sample only one cross-over point on the quality curve, these parameters are very sensitive to how quickly the power increases in the lowest part (first few nodes) of the bundle, but they are insensitive to the distribution of power above those points. In contrast, the I_2 parameter integrates the entire distribution of quality (area under quality curve) which gives a more robust behavior. This is particularly relevant for application to transients where sudden disturbances in local mass flow and power may occur near the inlet.

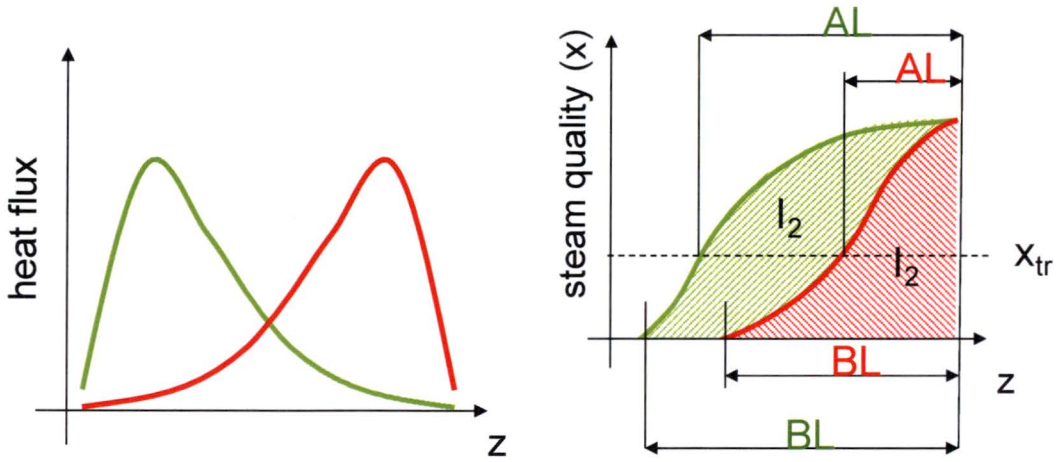

Figure 19-1 - Comparison of I_2 integral with Boiling Length (BL) and Annular Length (AL)

Eulerian to Lagrangian transformation

Challenges when modelling transient dryout

Analyzing dryout during a transient brings about several new complications that are not present in steady-state. The most difficult issue to handle is that several, if not all, parameters that could easily be described with single values in steady-state cannot be captured that way during a transient. The most obvious example is the mass flow rate, which in steady-state is constant along the channel, but can vary in a complicated way during a transient. Hence all the difficulties associated with the power distribution in steady-state will show up for the flow rate as well when analyzing transients.

Furthermore, parameters like the steam quality and flow rate, which are easily and accurately calculated in steady-state, require that complicated differential equations are solved during transients. Since some of these

equations include empirical or semi-empirical models (friction factors, void correlations) the input to the dryout model will be more uncertain compared to the steady-state case.

Transient dryout theory in Lagrangian coordinates

[

]^{a,c}

[

]^{a,c}

References

19-1 *Tech. Rep.* AECL-4927, Atomic Energy of Canada Ltd., "The effect of short flux spikes on the dryout power," Groeneveld, D., 1975.

19-2 *Tech. Rep.* R5076, AERE, "Studies of burnout in boiling heat transfer to water in round tubes with non-uniform heating," Bennett, A. W., Hewitt, G. F., Kearsey, H., Keeys, R. and Pulling, D., 1966.

19-3 PhD thesis, Imperial College, University of London, "Modeling of vertical annular and dispersed two-phase flows," Govan, A., 1990.

19-4 *Journal of Nuclear Science and Technology*, **40**, 6, pp. 383-, "Prediction of Critical Heat Flux in Annular Flow using a Film Flow Model," Okawa, T., Kotani, A., Kataoka, I. and Maito N., 2003.

19-5 *Nuclear Engineering and Design*, **229**, pp. 223-236, "Prediction of critical heat flux in annular regime in various vertical channels," Okawa, T., Kotani, A., Kataoka, I., and Naito, M., 2004.

20. RAI-SNPB-20 I_2 Limits

Provide additional justification on [

]^{a,c}

Response:

The D5 CPR correlation is a semi-local correlation where an axial dependence is only introduced via the R-factor. The purpose of the axial dependence of the R-factor is to better account for the local conditions for part-length rods (see Equation 5.3-2 and Figure 5.8). For typical conditions of a CPR limiting bundle the D5 CPR correlation [ ]^{a,c} As described in Section 5.4, a local I_2 model has also been developed, [

]^{a,c}

A truly local CPR correlation would need to explicitly account for the effects downstream of the spacers at discrete axial locations. Such detailed effects are modeled by mechanistic codes such as the MEFISTO code which has been used for benchmarking and validation of the D5 CPR correlation.

21. RAI-SNPB-21 Process for Generating Correlation Coefficients

Provide an overview of the manner in which the data was used to generate the correlation coefficients. Start with the initially chosen form and coefficients and detail how those coefficients were updated, when the rod constants and R-factors were initially calculated, and when they were updated, and conclude with the final form of the correlation's coefficients, the R factors, and the rod constants.

Response:

A least squares method was used to optimize the CPR correlation and R-factor coefficients by systematically minimizing the difference between the predicted and measured critical power for the [ ]^{a,c} dryout database obtained in FRIGG. The basis for this optimization was the variation of mass flux, system pressure, inlet subcooling, axial power profile, and radial rod power distribution studied in the FRIGG experiment. The fitting procedure is as follows.

[

]^{a,c}

22. RAI-SNPB-22 MEFISTO Analysis

The analysis performed with MEFISTO supported [

]^{a,c}

Response:

Subsequent to publication of Rev. 0 of WCAP-17794-P, during a recent FRIGG test with similar sub-bundle geometry and similar spacers as used in the original SVEA-96 Optima3 tests (same flow channel, same heater rods, same corner location of 1/3 part-length rod, same axial locations of spacers) the power on the 1/3 rod was increased until dryout was detected. A nearby full-length rod reached dryout simultaneously which allowed a direct comparison of predicted dryout margins for the two rod types at the same critical power condition. The D5 correlation predicted [

]^{a,c} This confirms that the dryout sensitivity constant for the 1/3 rod in the D5 model (e_1 of Equation 5.6-1) is conservative.

More background to the selection of the dryout sensitivity constant, e_1, is given below.

The use of maximum power experimentally achieved on the 1/3 rod was not sufficient to be able to cover the full range of operation with respect to power peaking on that rod. It was hence necessary to consider hypothetical test cases with higher rod power on the 1/3 rod and conservatively estimate the corresponding critical power. This estimation was performed using a mechanistic approach with the MEFISTO code. The code has been demonstrated to accurately predict the dryout performance for the SVEA-96 Optima3 dryout database (with standard deviation error < 5%). The part-length rods are explicitly modeled (with no additional empirical modeling). See, e.g., *Nuclear Engineering and Design*, **241**, pp. 2843-2858, C. Adamsson and J.-M. Le Corre, "Modeling and validation of a mechanistic tool (MEFISTO) for the prediction of critical power in BWR fuel assemblies," 2011.

In the MEFISTO analysis, the main empirical factor impacting the predicted critical power is the local enhancement of drop deposition downstream of each spacer grid. In the evaluation of the 1/3 rod dryout performance, a conservative [

]^{a,c} The dryout sensitivity constant, e_1, was then set conservatively to predict a critical power which is [ ]^{a,c} the predicted critical power by MEFISTO. Hence, the MEFISTO analysis allows setting the D5 dryout sensitivity constant for the 1/3 rod, while still quantifying an acceptable dryout margin to conservatively cover the calculation uncertainties.

Significant integral power on the 1/3 rod is typically only achieved at the beginning of the cycle when the power distribution is bottom peaked. At this time in the cycle, the Safety Limit Minimum CPR (SLMCPR) includes significant conservative margin since it is based on the more limiting condition near end of cycle when most rods come near the core minimum CPR.

For a limiting pressure transient that occurs late in cycle (when the control rods are almost fully withdrawn) the 1/3 rods have relatively low power since the core power shape is top-peaked. These fuel rods experience even lower power during the transient as the insertion of control rods during scram, and the associated void collapse, lead to an even more pronounced top-peaked power shape.

Furthermore, during normal operation, the power in the 1/3 rods is effectively protected by the Linear Heat Generation Rate (LHGR) limit. With the selected dryout sensitivity constant, e_1, [

]^{a,c}

23. RAI-SNPB-23 Validation Data

Data used to determine the correlation's predictive uncertainty (i.e., validation data) should not be used to train the correlation, as the correlation will predict training data with more accuracy than it would predict data it has never seen. Given that [

]^{a,c}

Response:

The database used for optimizing the D5 correlation coefficients was divided into two random subsets with [ ]^{a,c} This process was repeated 500 times. For each random trial, [

]^{a,c} The mean and standard deviation prediction errors were calculated separately for the training and validation datasets. The sample average results were well converged with 500 trials.

[

]^{a,c}

The demonstration presented above supports the decision of not splitting the database between training and validation sets. This decision was based on the robust nature of the D5 correlation formulation, having an exponential form with few regression coefficients, and its more physical modeling approach.

24. RAI-SNPB-24 Enforcement of the Computational Domain

Provide details which specify how the computational domain of the correlation is enforced. What happens if the code using the correlation attempts to apply it outside that domain?

Response:

If the D5 correlation is applied outside its limits of validity, the calling computer code will issue a warning message to the output. Per procedure, this would require the design engineer to investigate the conditions under which the range violation has occurred and take necessary actions to ensure conservatism of the calculation result. Normally, for the D5 correlation, the procedure involves confirming that it is not a limiting case, i.e., the corresponding sub-bundle has no realistic possibility of influencing the result of the calculation. Based on experience with the D5 correlation for European plants, range violation for applications to normal operation are rare and may only occur in cases of extreme local conditions where the (sub-)bundle in question is far from being CPR limiting for the core as a whole. An example is the situation of a very skewed radial power distribution caused by a deeply inserted control blade, possibly enhanced by a particular nuclear design used. This could, in extreme cases, result in the sub-bundle R-factor being slightly out of range for the sub-bundle closest to the control blade, due to the relatively higher power in the rods furthest away from the blade (i.e., the 2/3 length rods near the central water channel). Under such conditions the affected sub-bundle would operate at a much reduced total power due to the power suppression by the control blade, to an extent where the CPR margin is much greater than for an un-controlled bundle of the same nuclear design.

Range violation in high-power bundles is not expected for applications of the D5 correlation to normal or transient operation. Should it occur, the procedure would involve a conservative extrapolation of results obtained from slightly modified conditions where the correlation is applied within its limits. In any case, the robust mathematical form of the D5 correlation ensures a smooth variation of the results, without any sudden jumps or unexpected behavior, also outside the application limits.

25. RAI-SNPB-25 Sparse Region (1) in the Computational Domain

[

]^{a,c}

Response:

[

]^{a,c}

The negative dependence of critical quality on flow in the SVEA-96 Optima3 database is demonstrated in the figure below.

[a,b,c

]

A critical quality / mass flux trend analysis at dryout power was performed by considering [

]^{a,c}

When considering the relevant range of BWR core operation, the measured critical quality vs mass flux is plotted in the figure below, [

]^{a,c}

a,b,c

[

]a,c

a,b,c

Reference:
25-1 [

]a,c

26. RAI-SNPB-26 Sparse Region (1) in the Computational Domain

[

]^{a,c}

Response:

As presented under RAI-SNPB-25, [

]^{a,c} Hence, in the context of the present RAI, the question is whether to use a pressure dependent break-point in flow for the onset of this conservative treatment.

According to the data at 70 bar, the [

]^{a,c} Since the measured trends of critical quality with flow in the region [

]^{a,c}

It should also be mentioned that the detailed treatment in this interval of very low flow is of limited practical importance at off-rated pressure since it is highly unlikely that any limiting pressure transient can reach such low flow in BWR/2-6 or ABWR plants.

27. RAI-SNPB-27 Sparse Region (2) in the Computational Domain

[

]^{a,c}

Response:

[

]^{a,c}

It should also be mentioned that this interval of relatively high flow is of limited practical importance at off-rated low pressure since it is highly unlikely that any limiting pressure transient or accident condition (e.g., LOCA) reaches such conditions in BWR/2-6 or ABWR plants.

28. RAI-SNPB-28 Other Sparse Regions in the Computational Domain

[

]^{a,c}

Response:

(a) The D5 correlation predicts a critical power dependence of [

]^{a,c}

is also reflected in the data shown in Figures 4-11, 4-12, 4-17, 4-18, 4-23, and 4-24. A similar trend has been observed for previous fuel designs. [

]^{a,c}

(b-c) In addition, this answer addresses similar sparse regions for R-factor [ ]^{a,c} in the plots of R-factor versus pressure and inlet subcooling provided in response to RAI-SNPB-03.

The sparse regions are characterized by off-nominal conditions in mass flux, pressure or inlet subcooling, combined with an R-factor [ ]^{a,c} As explained in the response to RAI-SNPB-07, the relevant radial power distributions for a dryout limiting assembly are those accomplished by the nuclear design optimization, attempting to obtain a flat rod-wise CPR distribution in the un-controlled condition at the end of Gd depletion when the fuel reaches its maximum reactivity (k_{inf}). This is equivalent to minimizing the R-factor at the time of maximum reactivity. The example below shows such an optimized R-factor as a function of burnup for a case where maximum reactivity is reached around 10 MWd/kgU. The example confirms that the R-factor range below 1.06 is the relevant range for use of the D5 correlation to predict CPR margins for limiting assemblies in the core.

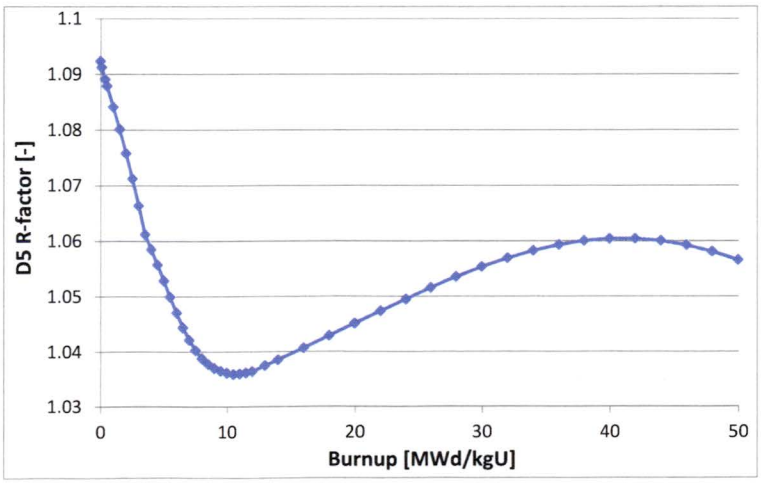

Figure 28-1 - D5 R-factor as a function of burnup

[

]^{a,c}

(d) Conditions of high R-factor are generally not limiting, as explained in the response to RAI-SNPB-07. The equivalence between optimizing nuclear design to achieve a flat rod CPR distribution, and minimizing the R-factor when the fuel is limiting, is given in the previous paragraph (b-c).

29. RAI-SNPB-29 Demonstrate Data Set Poolability

Provide analysis which demonstrate that the data from the three axial power distributions are poolable. This analysis should include a comparison of the mean, variances, and shape of the populations of the bottom-peaked, cosine, and top-peaked axial power shapes.

Response:

The mean and standard deviation prediction errors were calculated as shown in the table below for each subset of training data corresponding to a given axial power shape. The corresponding pooled mean and standard deviation prediction errors are [ ]^{a,c} according to Table 6-2. When including the conservative treatment of additional dryout data points for Rod 14 (see Section 6.3.1), the resulting final correlation mean and standard deviation are [ ]^{a,c} respectively (see Section 6.3.3). Hence, the final correlation standard deviation of [ ]^{a,c} conservatively bounds the results for all three axial power shapes. The [

]^{a,c}

a,c

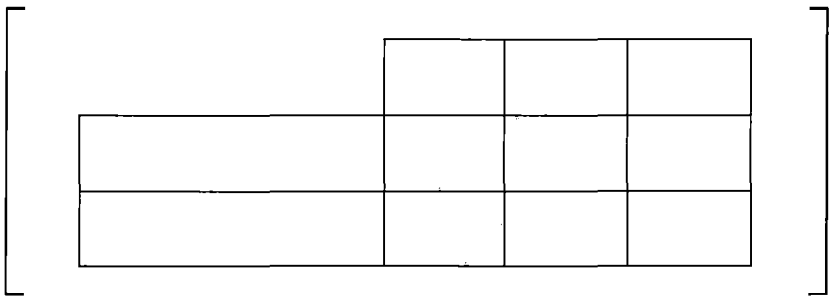

30. RAI-SNPB-30 Negative Bias

Provide a discussion on why not crediting the negative bias is conservative.

Response:

The mean prediction error, ε, is evaluated based on the definition in Equation 6-1. A negative value implies that, on average considering the entire database, the correlation predicts a critical power which is lower than the measured critical power.

It is possible to account for a non-zero mean prediction error of the CPR correlation in the safety evaluation by effectively shifting the Safety Limit Minimum CPR (SLMCPR). However, this is not done for the D5 correlation and, hence, the approach is conservative.

31. RAI-SNPB-31 Figures 4-9 and 4-10

In Figures 4-9 and 4-10 [ ]^{a,c}
Provide a further analysis of these figures.

Response:

Figures 4-9 and 4-10 are examples of how the D5 CPR correlation predictions compare with two small subsets of the database. These subsets are characterized by essentially two fixed radial power distributions [

]^{a,c} The choice of different subsets of this type would lead to different biases (positive or negative), consistent with the calculated error and standard deviation of the correlation.

32. RAI-SNPB-32 Degrees of Freedom

How many degrees of freedom were used in the analyses? [
]^{a,c}

Response:

[

]^{a,c}

33. RAI-SNPB-33 Transient Selection

Provide details on the transient forcing functions chosen. Justify how the forcing functions represent the limiting or most extreme AOOs in which the correlation will be applied for safety analysis.

Response:

The FRIGG transients were designed to effectively bound the limiting transients in all reactor types for which the SVEA-96 Optima3 fuel is intended to be used. These include Nordic ABB Generation 1-4 reactors, Siemens KWU reactors, GE BWR/2-6 reactors, and ABWR reactors. The limiting criteria to consider are the magnitude, rate and duration of flow reduction and power increase during the transient. Limiting transients in ABB Gen 3-4 and KWU plants with internal recirculation pumps are generally characterized by a fast and significant flow reduction, possibly combined with a moderate power increase. The BWR/2-6 plants currently operating in the US are generally limited by fast pressure increase transients, e.g., the Generator Load Rejection Without Bypass (LRNBP) event. Such transients are characterized by a fast power increase (due to reactivity insertion by void collapse), possibly combined with a moderate flow reduction. The transient behavior of an ABWR is intermediate, between BWR/6 and plants with internal pumps.

The FRIGG loop is designed to accommodate fast changes in both flow and power, individually or simultaneously. A fast pressure increase, however, cannot be accomplished due to the large volume. Instead, the consequences of the pressure increase on power and flow are simulated. **[**

][a,c] For US plants the characteristics of the power increase is of primary interest. Since the heat transfer characteristics of the FRIGG heater rods and reactor fuel rods differ somewhat, the time evolutions of the surface heat flux were calculated in both cases for comparison. For the impact on CPR the magnitude and duration of the power increase are more important than the rate of increase. It has been verified by considering various limiting transients in different plant types that the FRIGG transients indeed are representative and bounding.

34. RAI-SNPB-34 Figure 7-2

Will the D5 correlation be implemented in computer codes other than BISON-SLAVE? If so, provide the criteria which will be used to ensure an appropriate implementation.

Response:

Yes, the D5 CPR correlation will be implemented in the NRC-approved Westinghouse codes used for fuel and core analyses. Current examples include POLCA7, POLCA-T and GOBLIN, in addition to BISON.

The D5 CPR correlation relies on single-channel total mass and heat balance models only (i.e., mixture mass flow and enthalpy) and, as such, is independent of the thermal-hydraulic code used in steady-state, i.e., thermal equilibrium, analysis. Hence the derived statistical performance of the correlations is applicable to any steady-state application, for instance POLCA7 (regardless of the considered void correlation, subcooled boiling model or pressure drop models).

In the case of transient applications however, the non-equilibrium nature of the flow may lead to non-negligible differences between codes. Hence, the conservatism of the CPR correlation needs to be verified for every considered transient code.

New CPR correlations are normally incorporated into a Dryout Correlation Library Module (e.g., used by POLCA7 and POLCA-T), or directly implemented as a subroutine in the code (e.g., BISON and GOBLIN), following Westinghouse internal procedures for validation and verification of software changes. In the case of CPR correlations, this qualification is performed by modelling the FRIGG experiments that were utilized to validate the correlation, in the same way as shown in Section 7 for the BISON code. In this way, the validation of the code predictions against the FRIGG database provides the confirmation of its appropriate implementation. This process is documented, for future reference, in a Software Release Note for each code. The CPR correlation cannot be used in licensing applications before the corresponding Software Release Note has been issued.

Westinghouse's QA program for software releases is in compliance with the requirements in Appendix B to 10CFR Part 50 and has been audited by the NRC.

35. RAI-SNPB-35 Figure 7-2

Is the y-axis title for figure 7-2 correct?

Response:

The y-axis for Figure 7-2 should be "Relative Flow [-]".